Bioorganic Chemistry 92 (2019) 103297

Contents lists available at ScienceDirect

Bioorganic Chemistry

journal homepage: www.elsevier.com/locate/bioorg

# Targeted 8-hydroxyquinoline fragment based small molecule drug discovery against neglected botulinum neurotoxin type F

Ritika Chauhan[a], Vinita Chauhan[a], Priyanka Sonkar[a], Manorama Vimal[b], Ram Kumar Dhaked[a,*]

[a] Biotechnology Division, Defence Research & Development Establishment, Jhansi Road, Gwalior 474002, MP, India
[b] Synthetic Chemistry Division, Defence Research & Development Establishment, Jhansi Road, Gwalior 474002, MP, India

ARTICLE INFO

*Keywords:*
Botulinum neurotoxins (BoNTs)
8-Hydroxyquinoline (8-HQ)
Small molecule inhibitors (SMIs)
SNARE proteins
Fluorescence thermal shift (FTS)
Surface plasmon resonance (SPR)

ABSTRACT

*Objectives:* Botulinum neurotoxins are highly potent biological warfare agents. The unavailability of countermeasures against these neurotoxins has been a matter of extensive research. However, no clinical therapeutics has come to existence till date. The 8-hydroxyquinoline (8-HQ) scaffold is established privileged compound and its potential as drug candidate against BoNTs is recently being explored.

*Methods:* In present work, three course studies were performed involving *in silico*, *in vitro* and *in vivo* cascade to screen 8-HQ small molecule inhibitors against BoNT/F intoxication. ~800 molecules obtained from open repositories were screened *in silico* and commercially obtained twenty-four 8-HQ derived small molecule inhibitors were evaluated against rBoNT/F light chain through fluorescence thermal shift (FTS) assay. Selected compounds were further evaluated through endopeptidase assay. Further binding affinity analysis was done through surface plasmon resonance (SPR) based Proteon™ XPR 36 system. Finally, the *in vivo* efficacy of these compounds was evaluated in mice model.

*Results:* Three compounds NSC1011, NSC1014 and NSC84094 were found to be highly inhibitory after screening of 8-HQ compounds through FTS assay and endopeptidase assay. SPR based protein-small molecule interaction studies showed highest affinity binding of NSC1014 ($K_D$: 5.58E-06) with BoNT/F-LC. NSC1011, NSC1014, and NSC84094 displayed $IC_{50}$ of 30.47 ± 6.24, 14.91 ± 2.49 and 17.39 ± 2.74 μM, respectively, in endopeptidase assay. NSC1011 and NSC1014 displayed marked extension of survival time in mice model.

*Conclusion:* NSC1011 and NSC1014 have emerged as promising drug candidate against BoNT/F intoxication displaying higher potential than previously reported compounds.

## 1. Introduction

Botulinum neurotoxins (BoNTs), the most toxic substances known in nature, are listed category A biological threat agent of Centers for Disease Control and Prevention (CDC), USA [1]. BoNTs are classified into seven antigenically distinct serotypes denoted BoNT/A-G of that reported human cases are of A, B, E, and F; however, all serotypes may potentially intoxicate human [2]. BoNT intoxication results in neuroparalytic illness 'botulism', which has been majorly related to food poisoning [3]. These neurotoxins are produced by Gram-positive, rod shaped, motile, non-encapsulated, spore forming anaerobic bacteria *Clostridium botulinum* and strains of *C. butyricum* and *C. baratii* as ~150 kDa single polypeptide chain, that is cleaved by intrinsic or extrinsic proteases in to 100 kDa heavy chain (HC) comprising of ~50 kDa C-terminal cell receptor binding domain ($H_{CC}$), ~50 kDa *N*-terminal translocation domain ($H_{CN}$) and light chain (LC) of ~50 kDa acting as the catalytic domain displaying endopeptidase activity [2–4]. BoNT intoxication occurs in cholinergic nerve cells through receptor binding at the unmyelinated presynaptic membrane and internalization of LC through translocation [5]. The clinical presentation occurs after the $Zn^{2+}$ dependent metalloprotease activity of LC in the cytosol. It cleaves one of the Soluble *N*-ethylmaleimide sensitive factor Attachment Receptor (SNARE) proteins i.e. vesicle associated membrane protein (VAMP)/synaptobrevin, synaptosomal associated protein (SNAP-25), or syntaxin that prevents exocytosis of acetylcholine by inhibiting neurotransmitter vesicle fusion [6]. All toxinotypes inhibit

*Abbreviations:* BoNTs, botulinum neurotoxins; 8-HQ, 8-hydroxyquinoline; SMIs, small molecule inhibitors; SNARE proteins, soluble *N*-ethylmaleimide sensitive factor attachment receptor; VAMP, vesicle associated membrane protein; SNAP-25, synaptosomal associated protein-25 kDa; FTS assay, fluorescence thermal shift; SPR, surface plasmon resonance; FRET, fluorescence resonance energy transfer; RU, resonance unit; Ka, association constant; $K_d$, dissociation constant; $K_D$, equilibrium constant; MLD, minimum lethal dose

* Corresponding author.
*E-mail address:* rkdhaked@drde.drdo.in (R.K. Dhaked).

https://doi.org/10.1016/j.bioorg.2019.103297
Received 29 April 2019; Received in revised form 13 September 2019; Accepted 16 September 2019
Available online 17 September 2019
0045-2068/ 

acetylcholine release at neuromuscular junctions however intensity varies significantly due to their binding receptors and intracellular target proteins [7,8].

The ease with which they can be produced and disseminated, implicates their mass destructive potential and development of effective therapeutics is of high priority to counter bioterrorist attack. The use of antitoxin has been prevalent in past that reduces the severity of intoxication but unable to provide effective therapeutic solution [9–13]. Clinical use of BoNTs in various medical conditions i.e. neuralgia, migraine, spasticity and others, further complicates the situation. Recently, to overcome the shortcomings the research has been focussed on target based small molecule drug discovery. The advances in understanding and available solved structures of BoNTs with or without inhibitors have resulted in development of computational methods of drug designing [14,15]. Inhibiting metalloprotease activity through small molecules has been brought into light and numerous reports have been published ever since exploring the potential of small molecule inhibitors (SMIs) [16–29]. SMIs could act as potential drug, given their target specificity and ability to neutralize internalized LCs. Moreover, SMIs can prove highly effective medical countermeasure against BoNTs due to their conformational liberty and stability. The quinolinol based scaffold is one of screened potential drug candidates against BoNTs. Roxas-Duncan *et al.* reported the potential of 8-hydroxyquinolines (8-HQ) in inhibiting the metalloprotease activity of BoNT/A-LC and BoNT/A holotoxin [30]. Study was further followed by discovering more 8-HQ derivatives along with peptidic inhibitors [31]. In other study, 8-HQ compounds were presented as an attractive scaffold to design BoNT/A inhibitors through clinically approved Clioquinol and Chloroxine molecules that can be repurposed [32]. Further, Montgomery *et al.* first described the 8-HQ based SMIs against BoNT/B, C, E and F in *ex vivo* assay [33]. Fluorescence resonance energy transfer (FRET) has been employed to identify 8-HQ based inhibitors against BoNT/A through extensive mining of 4 different scaffolds [34]. Recently, quinolinol moieties derived structures against BoNT intoxication are further elucidated in three major studies [35–37]. Present study is focused on discovery of potential lead against lesser explored BoNT type F. It was performed by virtual high-throughput screening of open repositories focusing on 8-HQ, an excellent privileged scaffold possessing wide range of pharmacological applications and are reported multi-functional strong metal ion chelator. Our findings clearly signify the potential of 8-HQ scaffold in drug discovery and designing against BoNT/F intoxication by inhibition of $Zn^{2+}$ mediated metalloprotease activity.

## 2. Experimental section

### 2.1. Ethics statement

The care and maintenance of the animals was as per the guidelines of the Committee for Purpose of Control and Supervision of Experiments on Animals (CPCSEA), India. Animals were maintained under proper housing conditions and experimentation was carried out as per the approved guidelines of Institutional Animal Ethics Committee of Defence Research Development Establishment (DRDE), Gwalior.

### 2.2. Materials

HRP-labelled secondary antibodies, rabbit anti mouse immunoglobulins (P0161) & goat anti rabbit immunoglobulins (P0448) were purchased from DAKO, Denmark. Monoclonal anti-polyHistidine antibody produced in mouse (H1029), anti-glutathione-S-transferase (GST)–peroxidase conjugate antibody produced in rabbit (A7340), anti-vesicle-associated membrane protein-2 antibody produced in rabbit (V1389) were acquired from Sigma Aldrich, USA. Chemiluminescent peroxidise substrate (CPS350), and other required chemicals were obtained from Sigma Aldrich, USA. Novex prestained protein marker (LC5800) was purchased from Invitrogen, USA. The recombinant GST-VAMP-$2_{1–96}$ vector was kindly provided by Dr Christian Leveque INSERM, France. Test compounds for *in vitro* assays were obtained from the Drug Synthesis and Chemistry Branch, Developmental Therapeutics Program, Division of Cancer Treatment and Diagnosis, NCI, USA (Bethesda, MD) and ChemBridge Corporation, San Diego, CA, USA. RRGC a tetra-peptide inhibitor (> 95% pure) was synthesized from Bio Basic Inc. Ontario, Canada. The purities of compounds provided by NCI were > 99% and the compounds purchased from ChemBridge Corporation were > 95%.

### 2.3. Computer simulation studies

On the basis of previous findings, 8-HQ scaffold based molecules were used for similarity search and ~800 compounds were retrieved from from PubChem and ChemBridge databases. In an effort to identify potential inhibitors, high through-put *in silico* screening of compounds obtained was performed in order to identify potential BoNT/F inhibitors and docked on the active site of BoNT/F-LC (RCSB PDB: 2A8A). The protein structure was cleared of another ligand and reserved for small molecule interaction analysis. The flexible residues were taken as Glu228 and Tyr368 and the grid was set around −0.953, 2.791 & 20.889 for the specific active site interaction. Docking was performed as per AutoDock 4.2 protocol and scoring was done on the basis of minimum binding energy (kcal/mol) of protein-ligand complex formation [38]. The protein-small molecule interaction was viewed and analyzed using UCSF Chimera [39] and AutoDock 4.2. The LigPlot analysis was further performed to visualize the selected lead compounds interactions with the BoNT/F-LC amino acids.

### 2.4. In vitro assays

#### 2.4.1. Fluorescence thermal shift (FTS) assay

The 24 compounds obtained commercially were analysed through fluorescence thermal shift (FTS) screening with 50 μM inhibitor, 800 nM rBoNT/F-LC and 5x SYPRO Orange dye after optimization studies for determining the appropriate inhibitor and rBoNT/F-LC concentrations. The interaction curve through the dye was obtained by initiating the reaction as reported in our previous study [41].

#### 2.4.2. Endopeptidase assay

These 24 compounds were also tested for inhibition of rBoNT/F-LC enzymatic activity on rVAMP-2 through endopeptidase assay [40]. Reactions were performed in buffer at 37 °C where rBoNT/F-LC was taken at the concentration of 5 nM, substrate (rVAMP-2) at 500 nM and the small molecule compounds were initially taken at 250 μM. The products were resolved by electrophoresis on a 13% SDS-PAGE followed by western blotting and developed by ECL. The amount of uncleaved substrate and cleaved product were then estimated by densitometry (GS800, BioRad Laboratories, USA). The compounds with higher inhibitory potential as obtained were again analyzed at 100 and 50 μM concentrations. The experiments were performed at least thrice independently.

#### 2.4.3. Surface plasmon resonance (SPR) assay

The ProteOn™ XPR36 protein interaction array system from Bio-Rad Laboratories, USA was used for requisite interaction analysis. Simultaneous real-time analysis of six different concentrations/ligands could be done with six different/concentration analytes in 6X6 array format through XPR36 system. SPR analysis was performed by immobilizing rBoNT/F-LC as ligand at varied concentration (10.0, 5.0, 2.5, 1.0 and 0.5 μM) along with PBS as control for optimal binding on a GLM chip. The standard procedure was followed as per protocol reported elsewhere [41]. The small molecules NSC1011, NSC1012, NSC1014, NSC84087 and NSC84094 were taken as analytes at 10 μM concentrations prepared in phosphate buffered saline-tween 20, pH 7.4.

**Table 1**
Binding energies and inhibitory concentrations of small molecules analyzed *in vitro* as observed *in silico* through Autodock 4.2.

| Benzamide derivatives | | |
|---|---|---|
| S. no. | Name and score | Structure |
| **1** | **NSC297124**<br>N-(2-Oxo-5,5-diphenyl-tetrahydro-furan-3-yl)-benzamide<br>Molecular weight: 357.4<br>B.E.: −10.88 kcal/mol<br>Ki: 10.53 nM | 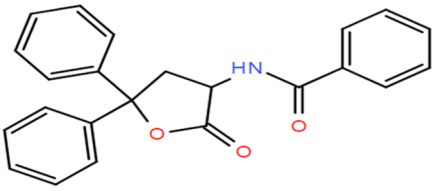 |
| **2** | **NSC201576**<br>3-Chloro-N-[(diphenyl-phosphinoyl)-furan-2-yl-methyl]-*N*-methyl-benzamide<br>Molecular weight: 449.87<br>B.E.: −10.33 kcal/mol<br>Ki: 26.99 nM | 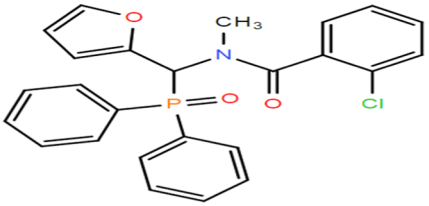 |
| **3** | **NSC36167**<br>N-[2-(Benzylidene-amino)-1,2-diphenyl-ethyl]-benzamide<br>Molecular weight: 404.5<br>B.E.: −11.67 kcal/mol<br>Ki: 2.8 nM | 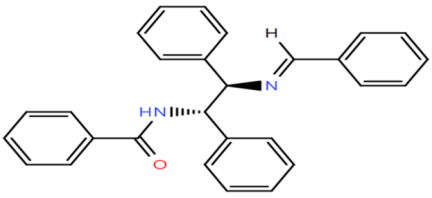 |
| **4** | **NSC157924**<br>N,N'-[(1,2-Diphenyl-1,2-ethanediyl)bis(imino-2,1-ethanediyl)]dibenzamide<br>Molecular weight: 506.64<br>B.E.: −10.23 kcal/mol<br>Ki: 31.57 nM | 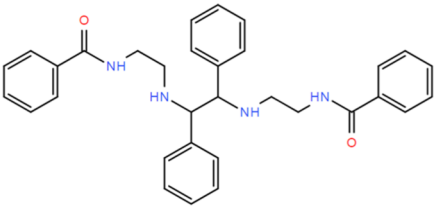 |

| Amines | | |
|---|---|---|
| S. no. | Name and Score | Structure |
| **1** | **NSC1006**<br>5-(2,2-Dimethyl-propyl)-5-methyl-imidazolidine-2,4-dione<br>Molecular weight: 184.24<br>B.E.: −7.86 kcal/mol<br>Ki: 1.72 μM | 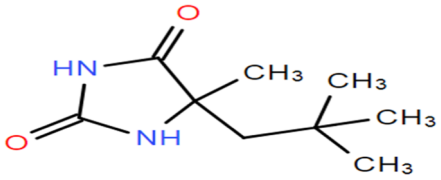 |
| **2** | **NSC1009**<br>3-Hydroxy-6-hydroxymethyl-2-(phenyl-phenylamino-methyl)-pyran-4-one<br>Molecular weight: 323.34<br>B.E.: −10.21 kcal/mol<br>Ki: 32.73 nM | 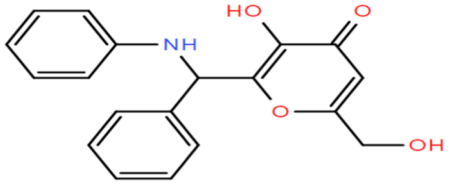 |
| **3** | **NSC1017**<br>2-[(3-Chloro-phenylamino)-phenyl-methyl]-3-hydroxy-6-hydroxymethyl-pyran-4-one<br>Molecular weight: 357.79<br>B.E.: −11.03 kcal/mol<br>Ki: 8.19 nM | 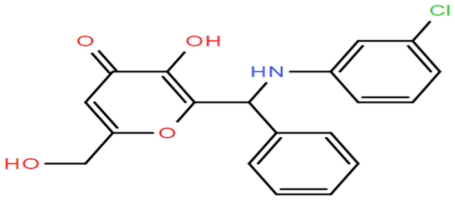 |
| **4** | **NSC1018**<br>N-(2,4-Dinitro-phenyl)-N'-(1-methyl-heptylidene)-hydrazine<br>Molecular weight: 308.33<br>B.E.: −7.22 kcal/mol<br>Ki: 5.12 μM | 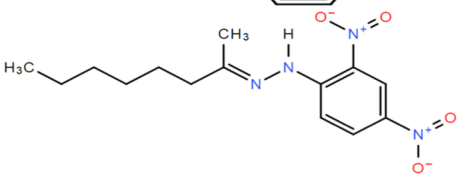 |

(*continued on next page*)

**Table 1** (*continued*)

| Amines | | |
|---|---|---|
| S. no. | Name and Score | Structure |
| **5** | **NSC84079**<br>{4-[1,3-Bis-(4-chloro-benzyl)-imidazolidin-2-yl]-phenyl}-bis-(2-chloro-ethyl)-amine<br>Molecular weight: 537.35<br>B.E.: −8.31 kcal/mol<br>Ki: 808.81 nM | 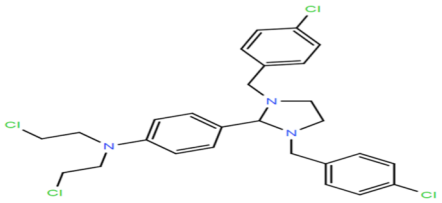 |
| **6** | **NSC84080**<br>{4-[1,3-Bis-(4-chloro-benzyl)-imidazolidin-2-yl]-3-methyl-phenyl}-bis-(2-chloro-ethyl)-amine<br>Molecular weight: 551.38<br>B.E.: −11.19 kcal/mol<br>Ki: 6.24 nM | 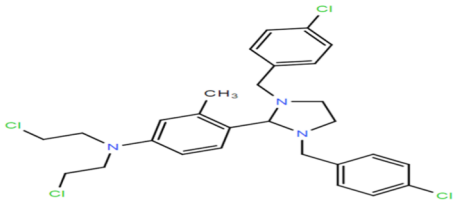 |
| **7** | **NSC84082**<br>4-{1,3-Bis[4-(*dimethylamino*)*benzyl*]-2-imidazolidinyl}-N,*N*-bis(2-chloroethyl)-3-methylaniline<br>Molecular weight: 568.62<br>B.E.: −9.27 kcal/mol<br>Ki: 160.8 nM | 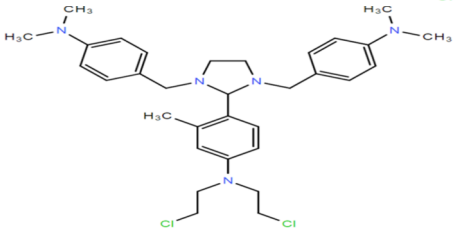 |
| **8** | **NSC84083**<br>[3-(Cyano-phenyl-methyl)-2-hexyl-tetrahydro-pyrimidin-1-yl]-phenyl-acetonitrile<br>Molecular weight: 400.56<br>B.E.: −12.44 kcal/mol<br>Ki: 3.04 nM | 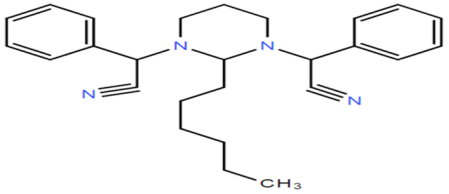 |
| **9** | **NSC84085**<br>{3-[Cyano-(4-methoxy-phenyl)-methyl]-2-phenyl-tetrahydro-pyrimidin-1-yl}-(4-methoxy-phenyl)-acetonitrile<br>Molecular weight: 452.55<br>B.E.: −11.73 kcal/mol<br>Ki: 2.54 nM | 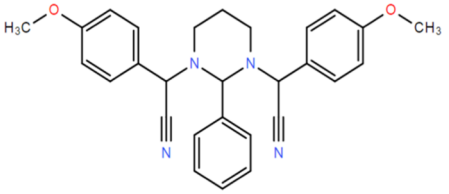 |

| 8-hydroxyquinolines | | |
|---|---|---|
| S. no. | Name and Score | Structure |
| **1** | **NSC1008**<br>7-(Phenyl-phenylamino-methyl)-quinolin-8-ol<br>Molecular weight: 326.39<br>B.E.: −11.05 kcal/mol<br>Ki: 7.97 nM | 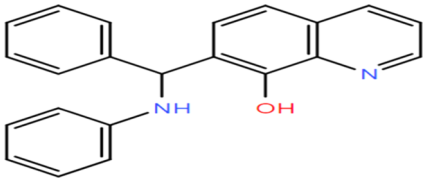 |
| **2** | **NSC1010**<br>7-[(4-Nitro-phenylamino)-phenyl-methyl]-quinolin-8-ol<br>Molecular weight: 371.39<br>B.E.: −10.98 kcal/mol<br>Ki: 8.96 nM | 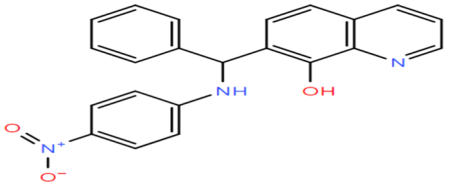 |
| **3** | **NSC1011**<br>**4-{[(8-Hydroxy-quinolin-7-yl)-phenyl-methyl]-amino}-benzoic acid**<br>Molecular weight: **370.4**<br>B.E.: −9.98 kcal/mol<br>Ki: 48.05 nM | 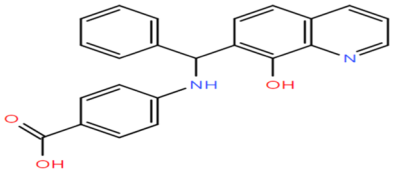 |

(*continued on next page*)

**Table 1** (*continued*)

| 8-hydroxyquinolines | | |
|---|---|---|
| S. no. | Name and Score | Structure |
| **4** | **NSC1012**<br>2-{[(8-Hydroxy-quinolin-7-yl)-phenyl-methyl]-amino}-benzoic acid<br>Molecular weight: 370.4<br>B.E.: −10.4 kcal/mol<br>Ki: 23.99 nM | 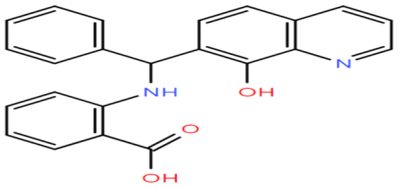 |
| **5** | **NSC1013**<br>7-[(4-Nitro-phenyl)-phenylamino-methyl]-quinolin-8-ol<br>Molecular weight: 371.39<br>B.E.: −10.33 kcal/mol<br>Ki: 26.7 nM | 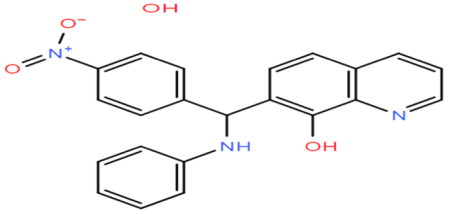 |
| **6** | **NSC1014**<br>**7-[(4-Methyl-pyridin-2-ylamino)-phenyl-methyl] -quinolin-8-ol**<br>Molecular weight: **341.41**<br>B.E.: −10.73 kcal/mol<br>Ki: 13.61 nM | 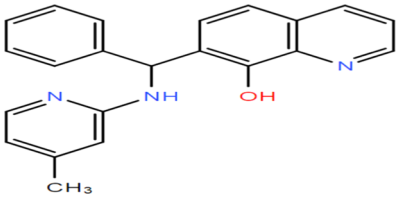 |
| **7** | **NSC1015**<br>2-{[(8-Hydroxy-quinolin-7-yl)-phenyl-methyl]-amino}-benzoic acid ethyl ester<br>Molecular weight: 398.45<br>B.E.: −11.28 kcal/mol<br>Ki: 5.35 nM | 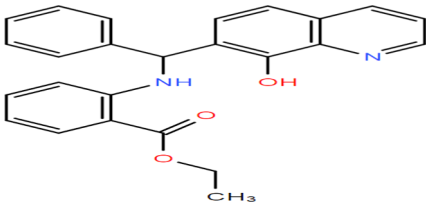 |
| **8** | **NSC66811**<br>2-Methyl-7-(phenyl-phenylamino-methyl)-quinolin-8-ol<br>Molecular weight: 340.42<br>B.E.: −10.21 kcal/mol<br>Ki: 32.68 nM | 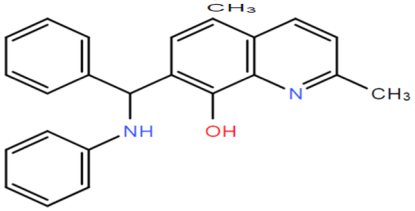 |
| **9** | **NSC66812**<br>2-{[(8-Hydroxy-2-methyl-quinolin-7-yl)-phenyl-methyl]-amino}-benzoic acid methyl ester<br>Molecular weight: 398.45<br>B.E.: −10.75 kcal/mol<br>Ki: 13.24 nM | 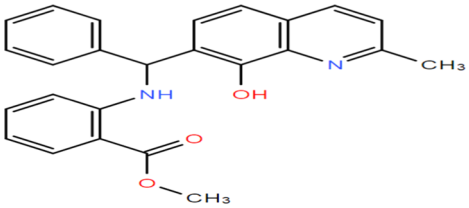 |
| **10** | **NSC84086**<br>7-[(2-Bromo-phenylamino)-phenyl-methyl]-quinolin-8-ol<br>Molecular weight: 405.29<br>B.E.: −10.77 kcal/mol<br>Ki: 12.72 nM | 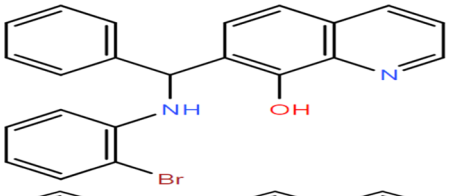 |
| **11** | **NSC84087**<br>7-[(2-Methoxy-phenylamino)-phenyl-methyl]-quinolin-8-ol<br>Molecular weight: 356.42<br>B.E.: −9.87 kcal/mol<br>Ki: 58.29 nM | 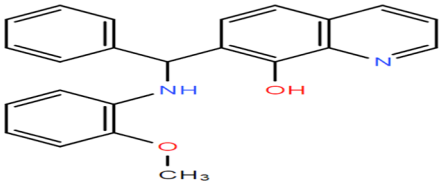 |

(*continued on next page*)

**Table 1** (*continued*)

| 8-hydroxyquinolines | | |
|---|---|---|
| S. no. | Name and Score | Structure |
| **12** | **NSC84090**<br>7-[(4-Chloro-phenylamino)-phenyl-methyl]-quinolin-8-ol<br>Molecular weight: 360.84<br>B.E.: −11.28 kcal/mol<br>Ki: 5.39 nM | 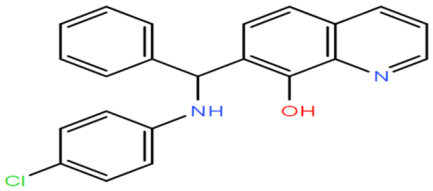 |
| **13** | **NSC84092**<br>7-[(Naphthalen-1-ylamino)-phenyl-methyl]-quinolin-8-ol<br>Molecular weight: 376.45<br>B.E.: −11.53 kcal/mol<br>Ki: 3.54 nM | 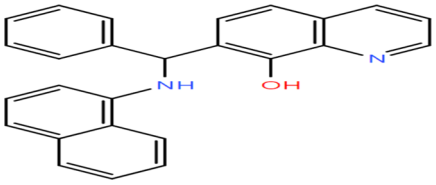 |
| **14** | **NSC84093**<br>7-(Phenyl-p-tolylamino-methyl)-quinolin-8-ol<br>Molecular weight: 340.42<br>B.E.: −10.97 kcal/mol<br>Ki: 9.13 nM | 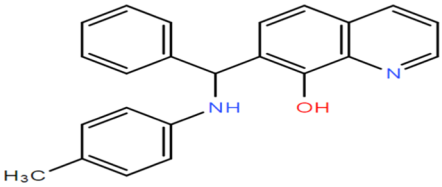 |
| **15** | **NSC84094**<br>**7-[Phenyl-(pyridin-2-ylamino)-methyl]-quinolin-8-ol**<br>Molecular weight: **327.38**<br>B.E.: −11.22 kcal/mol<br>Ki: 5.95 nM | 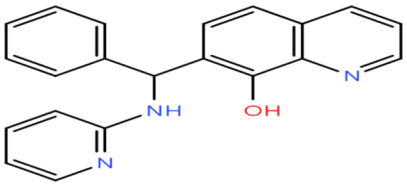 |
| **16** | **NSC84095**<br>7-[(4,6-Dimethyl-pyridin-2-ylamino)-phenyl-methyl]-quinolin-8-ol<br>Molecular weight: 355.43<br>B.E.: −11.62 kcal/mol<br>Ki: 3.05 nM | 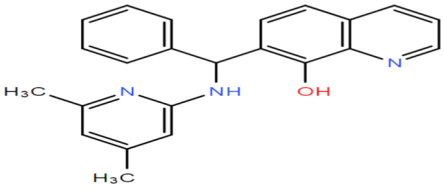 |
| **17** | **NSC84096**<br>7-[Phenyl-(quinolin-8-ylamino)-methyl]-quinolin-8-ol<br>Molecular weight: 377.44<br>B.E.: −10.53 kcal/mol<br>Ki: 19.05 nM | 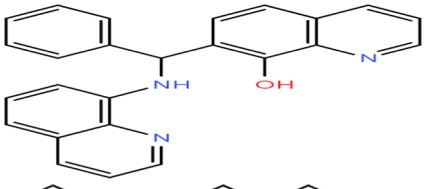 |
| **18** | **NSC84097**<br>2-Methyl-7-(phenylamino-pyridin-4-yl-methyl)-quinolin-8-ol<br>Molecular weight: 341.41<br>B.E.: −11.17 kcal/mol<br>Ki: 6.48 nM | 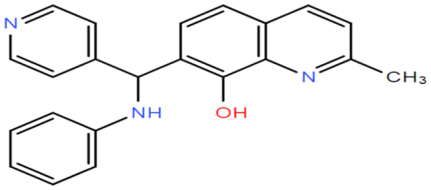 |
| **19** | **CB7969312**<br>5-Chloro-7-[(4-ethoxy-phenyl)-(pyridin-3-ylamino)-methyl]-quinolin-8-ol<br>Molecular weight: 405.88<br>B.E.: −10.61 kcal/mol<br>Ki: 16.76 nM | 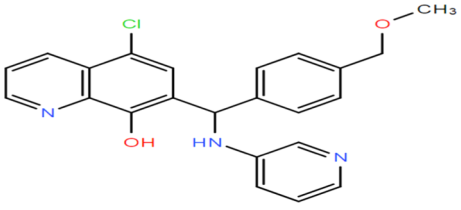 |

(*continued on next page*)

**Table 1** (*continued*)

| 8-hydroxyquinolines | | |
|---|---|---|
| S. no. | Name and Score | Structure |
| **20** | **CB7967495**<br>7-[(Pyridin-3-ylamino)-(4-trifluoromethyl-phenyl)-methyl]-quinolin-8-ol<br>Molecular weight: 395.38<br>B.E.: −10.49 kcal/mol<br>Ki: 20.62 nM | 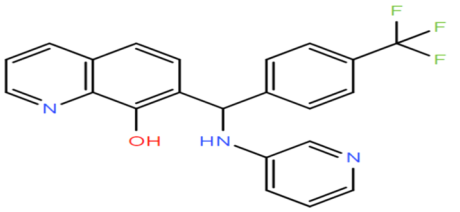 |
| **21** | **CB6377128**<br>7-[(4-Methylsulfanyl-phenyl)-(pyridin-2-ylamino)-methyl]-quinolin-8-ol<br>Molecular weight: 373.47<br>B.E.: −10.65 kcal/mol<br>Ki: 15.72 nM | 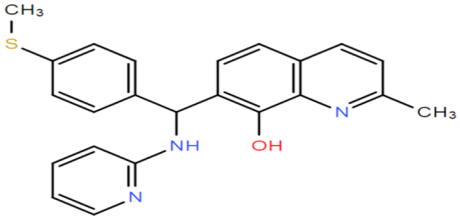 |
| **22** | **CB7925339**<br>5-Chloro-7-[(pyridin-2-ylamino)-(4-vinyloxy-phenyl)-methyl]-quinolin-8-ol<br>Molecular weight: 403.86<br>B.E.: −10.46 kcal/mol<br>Ki: 21.63 nM | 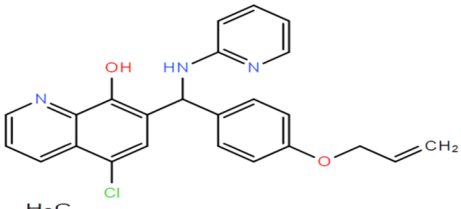 |
| **23** | **CB6378306**<br>7-[(3-Bromo-4,5-dimethoxy-phenyl)-(pyridin-2-ylamino)-methyl]-quinolin-8-ol<br>Molecular weight: 466.33<br>B.E.: −11.86 kcal/mol<br>Ki: 2.02 nM | 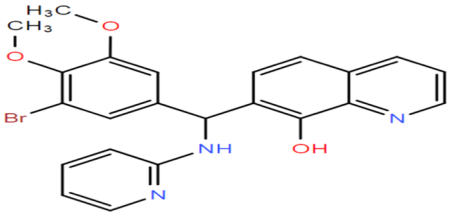 |
| **24** | **CB6376015**<br>7-[Benzo[1,3]dioxol-5-yl-(6-methyl-pyridin-2-ylamino)-methyl]-quinolin-8-ol<br>Molecular weight: 385.42<br>B.E.: −9.71 kcal/mol<br>Ki: 76.66 nM | 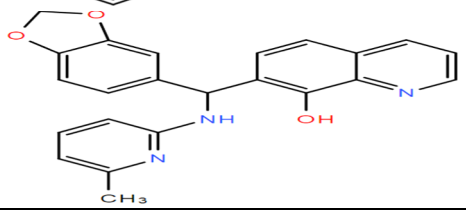 |

The baseline correction was performed against NSC66812 as negative control for determination of significant resonance or response unit (RU) values for the inhibitors. The immobilization at 2.5 μM rBoNT/F-LC was taken as optimum and considered for further analyte interaction analysis. All the experiments were performed at 25 °C. The sensorgram data obtained were analyzed using ProteOn Manager 3.1 software and fitted to the simplest Langmuir 1:1 interaction model.

### 2.4.4. $IC_{50}$ determination

Selected three compounds NSC1011, NSC1014, and NSC84094 were analyzed through endopeptidase assay to determine effective half maximal inhibitory concentration ($IC_{50}$) value. Ten concentrations 100, 75, 50, 25, 12.5, 6.25, 3.125, 1.5625, 0.78125, and 0.390625 μM of the respective small molecules were used for the estimation.

### 2.4.5. Hemolysis assay

The *in vitro* hemolysis assay was further conducted according to Sathler and collaborator [42] to determine hemoglobin release in the plasma upon SMIs exposure. Blood was obtained from healthy human subject. Erythrocytes were washed 3 times with PBS (pH 7.4) by centrifugation (500*g*). The compounds at 100 and 10 μM were incubated with the erythrocyte suspension for 3 h at 37 °C. The lysis of the erythrocytes and the release of hemoglobin were determined from the optical density of the supernatant at 540 nm. Triton X-100 (1%) was used as positive control that provided complete hemolysis. Assay was performed in triplicates. The percent hemolysis is calculated using the following formula:

$$\text{Percent hemolysis} = 100 \times [(A_{540}\text{sample} - A_{540}\text{negative control}) \div (A_{540}\text{positive control} - A_{540}\text{negative control})]$$

### 2.5. Mouse protection assay

Female Balb/c mice were used for *in vivo* evaluation and in all treatments intraperitoneal route (ip) of administration was adopted for mouse protection assay. Two compounds NSC1011 and NSC1014 were tested for their protection in mouse model; animals were divided into five groups of five animals each for every compound. Toxin alone treated group was administered as single dose of 5X MLD of BoNT/F. In second group, mice were given *in vitro* neutralized premixed solution of toxin and compounds after 1 h incubation at RT. In third group, animals were treated with compounds 1 h prior to injection of toxin

(prophylactic). Animals of fourth group received toxin and after 1 h compounds were injected (therapeutic). Control animals received the same volume of PBS as the experimental group. For all treatment a single dose of 100 µl of 25 mM compounds in DMSO was used. Three independent studies were performed.

## 3. Results & discussion

### 3.1. Computer simulation analysis

The introduction of virtual screening saves time and efforts on *in vitro* unproductive results. We applied this approach towards discovering and/or designing to identify potential molecules for BoNT/F inhibition. On the basis of chelating property 8-HQ derived molecules along with other chelating agents such as amines and benzamides were screened for finding effective agent (Table 1). Also 8-HQ scaffold based molecules are important 'privileged structures' that can be exploited as inhibitors of a diverse range of targets [43]. The 8-HQ based molecules have been reported in previous studies for their potential as specific lead compounds against BoNT intoxication. Similarity search was carried out and ~800 8-HQ compounds were retrieved from open repositories which were screened using AutoDock 4.2 against BoNT/F-LC. The binding energies of screened (twenty-four) compounds selected for further *in vitro* analysis varied from −11.86 to −9.71 kcal/mol and inhibitory concentration (Ki) values were from 2.02 to 76.66 nM. The energy results were ranked according to the binding energy which included the intermolecular energy and the torsional terms and Ki. Upon docking 8-HQ derivatives NSC1008, NSC1010, NSC1011, NSC1012, NSC1013, NSC1014, NSC1015, NSC84080, NSC84083, NSC84085, NSC84087, NSC84094, NSC84095, CB7969312, CB7887535 and CB6376015 were found to be the best molecules on the basis of Ki values and binding energies (Table 1). These molecules interact with the amino acid residues of signature metalloprotease active site His227; Glu228; His231; Arg365; Tyr368 and Tyr372 in close proximity with the metal ion ($Zn^{2+}$) depicting effective binding with BoNT/F-LC [44]. Compound NSC84094 is already reported inhibitor of BoNT/A and varies from NSC1014 in only one methyl substitution in pyridine ring at c-4, which provably increases the activity of the compound against BoNT/F.

The extensive simulation data of only three compounds NSC1011, NSC1014 and NSC84094 is hereby discussed. These compounds displayed promising outcome in biological assays including *in vivo* protection experiments in subsequent studies. The compounds in all the confirmations docks in the same cleft as observed in Fig. 1a–c. The interaction of these three compounds in the docked position with the BoNT/F-LC was observed and showed in the Fig. 2. The compounds NSC1011 (cyan), NSC1014 (purple) and NSC84094 (pink) shows the interaction in the active site in close proximity with the $Zn^{2+}$ along with the active site residues Ser165, Cys166, His227, Glu266, Arg365 and Tyr368. This suggests the directed fit of these molecules in the active site. The molecules, however in the same active site interacts in different confirmations which provides them specific binding and inhibitory potential (Fig. 3a(i-iii)). The LigPlot analysis of two compounds NSC1011 and NSC1014 displays their interaction with the specific amino acid residues (Fig. 3b(i-ii)). The common amino acids that are observed in both protein-small molecule interactions are Phe163, Ser165 and Glu228 (Fig. 3biii). The highly specific and targeted interaction of these compounds with the BoNT/F-LC along with low Ki values suggests their firm interaction that is validated in further *in vitro* studies. The pdb files used for SMI- BoNT/F-LC interaction

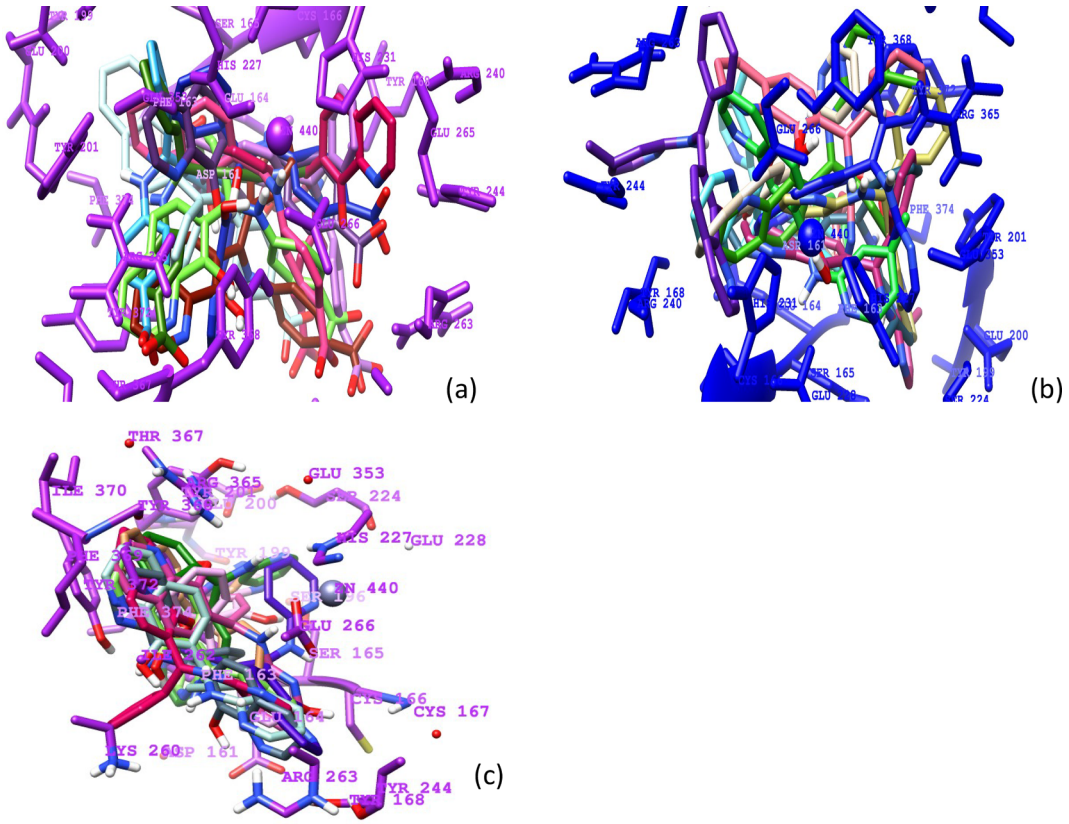


**Fig. 1.** The representative image as observed in UCSF Chimera in the active site of the BoNT/F-LC in 10 different confirmations of (a) NSC1011, (b) NSC1014 and (c) NSC84094. The interaction of all the confirmations can be observed in the fixed pocket signifying channelled interaction of the SMIs.

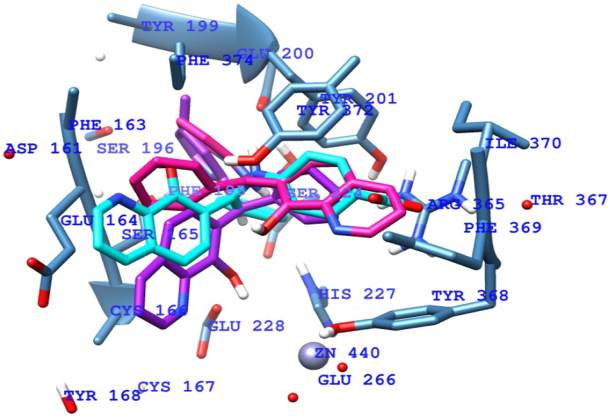


**Fig. 2.** The compounds NSC1011 (cyan), NSC1014 (purple) and NSC84094 (pink) shows the interaction in the active site in close proximity with the $Zn^{2+}$ along with the amino acids Ser165, Cys166, His227, Glu266, Arg365 and Tyr368.

analysis are provided in supporting information (FLcNSC1011.pdb, FLcNSC1014.pdb and FLcNSC84094.pdb).

### 3.2. Fluorescence thermal shift (FTS) assay

The *in silico* screening provided us with over 80 molecules while we were able to obtain only twenty-four 8-HQ compounds commercially for further *in vitro* analysis. Interaction between small molecule and BoNT/F-LC protein plays a key role in determination of their inhibitory potential. Primary screening of compounds was performed by FTS assay that quantifies the change in thermal denaturation temperature of a protein under varying conditions. Its functioning is conceptualized by effect of small molecule interaction on protein stability that increases melting temperature which could be analyzed using an environment sensitive fluorescent dye. With increase in temperature, unfolding of protein takes place and the fluorescent dye act as probe (SYPRO Orange), interact with the hydrophobic patches of unfolded rBoNT/F-LC thus providing high fluorescence upon binding [45]. FTS analysis serves us as platform for high through-put screening where interaction of selected 8-HQ compounds with the in house produced rBoNT/F-LC was studies [40]. The shift in the melting temperature ($\Delta Tm$) signifies the binding affinity of small molecule in groove of BoNT/F-LC making it stable (Fig. 4a). In general, the $> +2.0\,^{\circ}C$ shift in melting temperature ($\Delta Tm$) upon binding of molecules is considerable for further analysis. Among these compounds maximum shift in $\Delta Tm$ was recorded with NSC1010 (4.10 °C) followed by NSC1011 (3.85 °C), CB7925339 (3.54 °C), NSC1014 (3.53 °C), NSC1013 (3.52 °C), NSC84087 (3.30 °C), NSC1012 (2.95 °C), NSC84094 (2.28 °C), and NSC1015 (2.10 °C) as presented in Fig. 4b. The results obtained through FTS assay have been confirming the virtual simulations by affirming the compounds.

### 3.3. In vitro endopeptidase assay

*In vitro* endopeptidase assay was performed for observing appropriate inhibitory potential of the compounds using in house produced rBoNT/F-LC and rVAMP-2 [40]. Initially inhibition was studied at

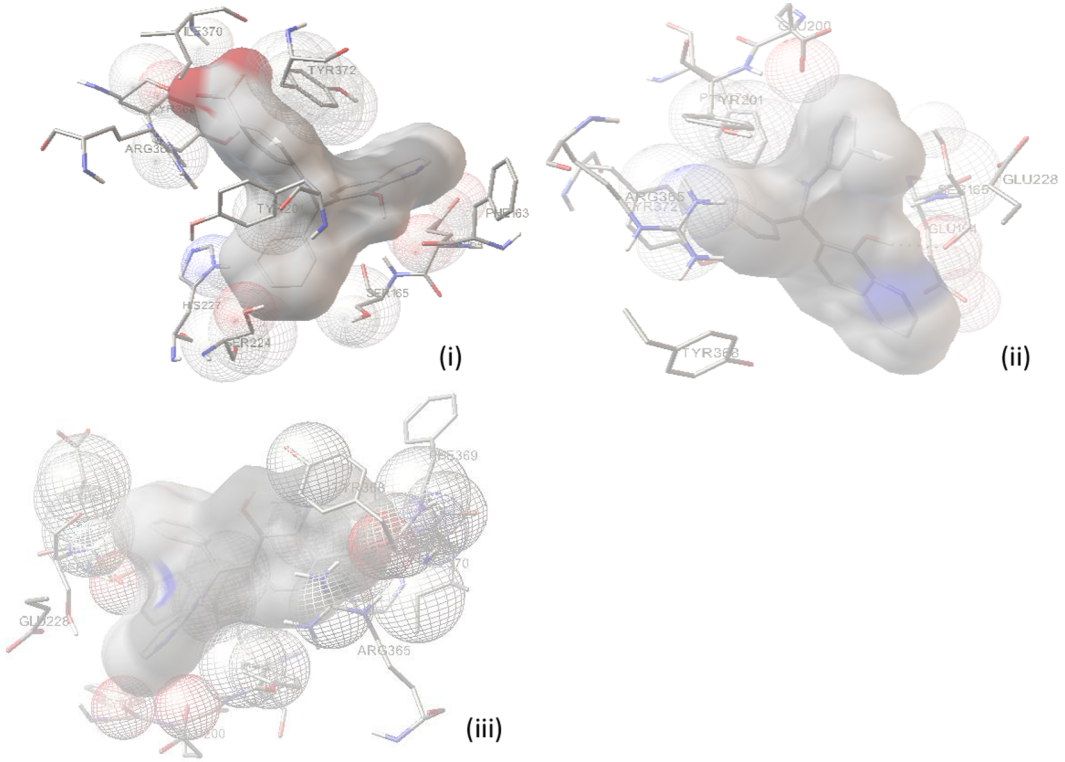


**Fig. 3a.** Interaction of SMIs with the active site of BoNT/F-LC in the firmest confirmation representing site specific proximal binding. (i) **NSC1011,** Binding energy of −10.04 and Ki of 43.69 nM. It interacts by forming hydrogen bonds with Arg263, Lys260, Ser165, Tyr368 and Tyr372. The formation of hydrogen bond is with paracarboxylic group, oxygen atom of quinolinol and –NH group showing the widespread interaction of the compound with the active moiety. Other interactions as observed include pi-pi interactions of Phe163 and Tyr368 with quinolinol ring and cation-pi interaction of Lys260 with benzoic acid ring (ii) **NSC1014,** Binding energy of −10.73 and Ki 13.61 nM. The hydrogen bond formation is not that much prevalent in interaction of NSC1014 and only one hydrogen bond observed between Cys166 with –OH group of quinolinol. The other interactions that have been observed are cation-pi interaction of Arg365 and pi-pi interaction of Tyr372 with the pyridine ring of the molecule and (iii) **NSC84094** also interacts with the BoNT/F-LC with high binding energy of −11.22 and Ki of 5.95 nM. The compound forms hydrogen bond with Tyr368 through the oxygen atom of quinolinol ring and Ser165 with phenyl oxygen of the molecule. The quinolinol ring also forms pi-pi interaction with Tyr372 and Phe374.

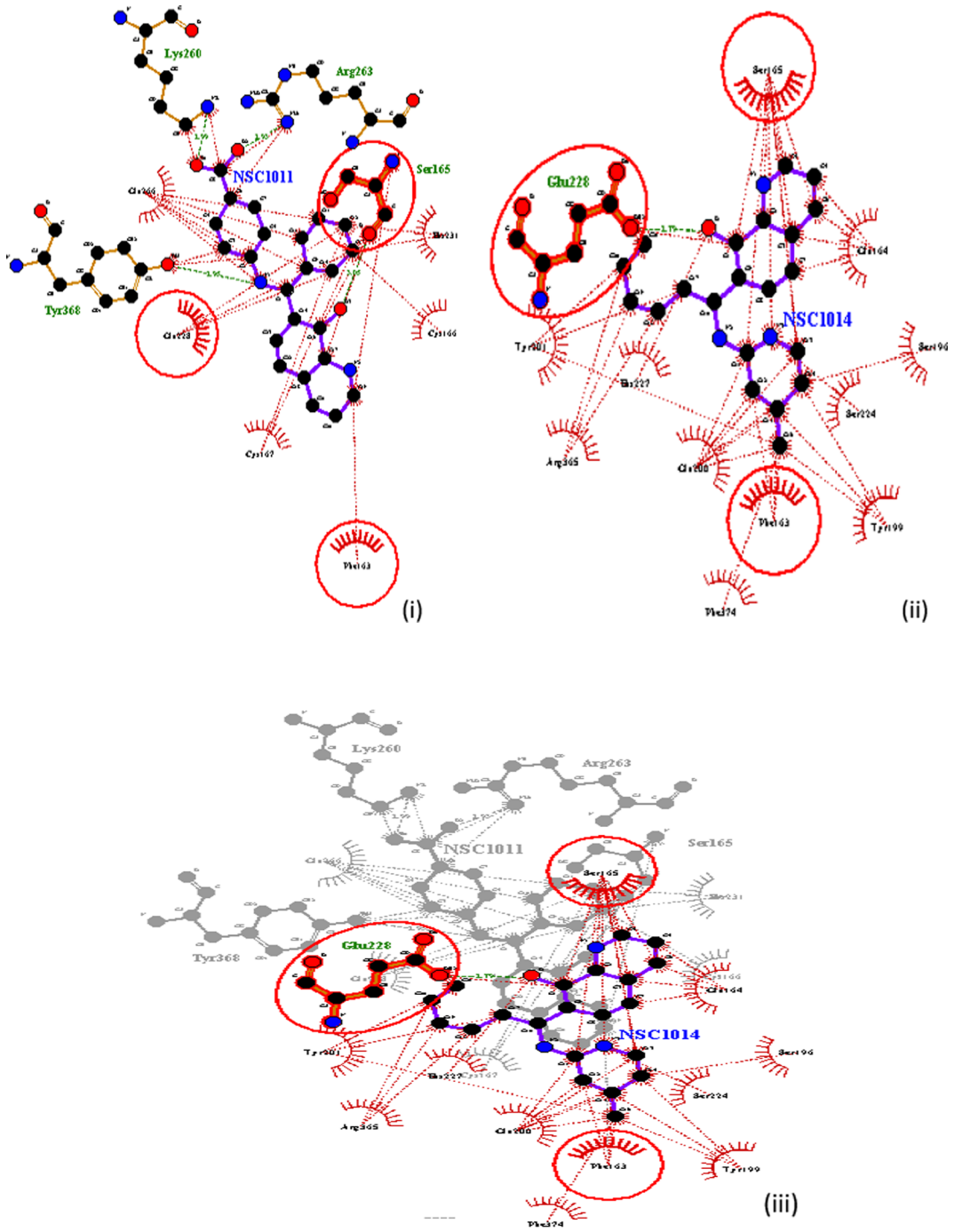


**Fig. 3b.** The LigPlot representative image displaying interaction of (i) **NSC1011** where it can be observed in targeted binding pocket interacting with very specific amino acids Ser165, Glu228 and Tyr368 along with others. (ii) **NSC1014** displays interaction in the targeted pocket interacting with Ser165 and Glu228 among others. (iii) The overlapped interaction displays the amino acids playing role in both of the protein-small molecule interaction i.e. Phe163, Ser165 and Glu228.

250 μM concentrations of the molecules and NSC1011, NSC1012, NSC1014, NSC1015, NSC84086, NSC84087, NSC84090, NSC84092, NSC84094, NSC84095 and CB7969312 were found to be potential inhibitors (Fig. 5a and b). The molecules which were active at higher concentration (250 μM) were analysed at subsequently at 100 and 50 μM concentrations. It was observed that three molecules NSC1011, NSC1014 and NSC84094 displayed complete inhibition at 100 μM concentration with CB7969312 showing 80 ± 2% while NSC84087 was displaying around 60 ± 2% inhibition (Fig. 6a and b). CB7969312 has been already tested in *ex-vivo* assay against BoNT/F [33]. The compounds found effective in the study showed higher inhibitory potential than CB7969312 proving the significant finding against BoNT/F intoxication. Rest of the compounds displayed either lower or no inhibition at 100 μM. NSC1011, NSC1014, and NSC84094 were found most active on the basis of *in silico* and two *in vitro* analyses i.e. FTS and endopeptidase assays.

### *3.4. Surface plasmon resonance analysis of protein-small molecule interaction*

SPR biosensor based assay was further performed to evaluate interaction between the selected small molecules and rBoNT/F-LC. The advance analysis was performed on ProteOn™ XPR36 system for SPR based protein-small molecule binding kinetics. The GLM chip based on

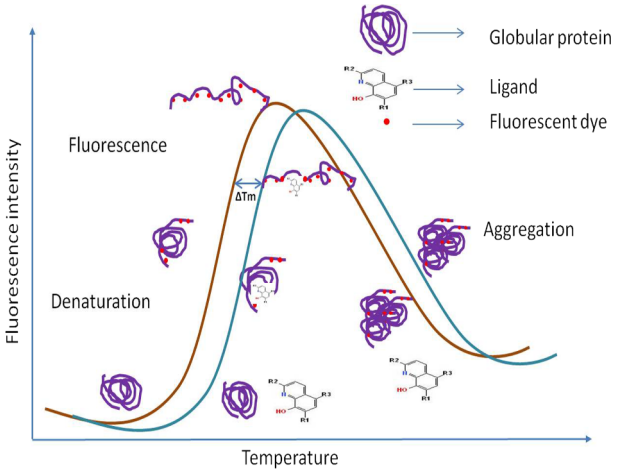


**Fig. 4.** (a) Schematic representation of fluorescence thermal shift assay of globular protein in absence and presence of a ligand with environment sensitive dye. In absence of ligand, the protein unfolds by increase in temperature leading to binding of the dye in hydrophobic moieties providing specific fluorescence. In presence of a ligand, on protein unfolding the ligand binds in the specific groove of the protein providing increased stability and thus increasing the temperature of protein unfolding. This change in temperature is the acquired thermal shift which signifies protein and small molecule interaction. (b) Fluorescence based thermal shift assay of selected SMIs as displayed in the graph. The SYPRO Orange dye was taken as the probe for determination of thermal shift due to increase or decrease of protein stability at 50 μM SMIs concentration.

amine coupling chemistry was used for immobilization of native purified rBoNT/F-LC protein (supplementary data; Fig. 1). The protein-small molecule interaction is measured by change of incident angle due to interaction between ligand and analyte through resonance unit (RU). Sensorgrams sensitively record this shift depicting the interaction which gradually returns to baseline on protein removal. In SPR based studies the reversible attachment and detachment of the molecule is monitored in terms of association and dissociation constants providing significant equilibrium analysis. The effective binding of selected 8-HQ small molecules even at lower concentration of rBoNT/F-LC signifies the directed and very specific interaction of these compounds. The association and dissociation kinetics in the term of Ka (association constant, $M^{-1}s^{-1}$), $K_d$ (dissociation constant, $s^{-1}$) and $K_D$ (equilibrium constant, M) is used for quantification of interaction. $K_d$ is presented as the concentration of inhibitor needed to inhibit 50% of activity of the rBoNT/F-LC. $K_D$ is determined as $K_d$/Ka and is inversely proportional to affinity between the protein and small molecule. NSC66812 which did not provide much of inhibition in endopeptidase assay and was rejected in thermal shift assay was clearly identifying the significant difference in $K_D$ among the reactive and non-reactive compounds in SPR assay also. The $K_D$ values as presented in Table 2 and is lowest in NSC1014 (0.558 μM) followed by NSC84094 (4.79 μM), NSC1011 ($3.14 \times 10^3$ μM), NSC84087 ($3.43 \times 10^3$ μM) and NSC1012 ($3.54 \times 10^3$ μM) (Fig. 7a–c). Negative control NSC66812 which has not displayed significant result in endopeptidase assay was found to exhibit the highest $K_D$.

### 3.5. $IC_{50}$ estimation through endopeptidase assay

The $IC_{50}$ of NSC1011, NSC1014 and NSC84094 for their potential drug candidature were then determined by constructing a dose-response curve to examine the antagonistic effect of these compounds on the rBoNT/F-LC activity. The $IC_{50}$ values thus determined has been used for comparative potency of the selected small molecules. Although, $IC_{50}$ is not direct indication of inhibitor affinity and interaction it can be related to the inhibitory potential in competitive inhibition by the Cheng-Prusoff equation [46]. Experimental Ki values of three compounds were calculated using this method considering the substrate concentration (r-VAMP-2) as required for rBoNT/F-LC metalloprotease activity as determined in our previous work [40]. The $IC_{50}$ of NSC1014 was found to be minimum at 14.91 ± 2.49 μM followed by NSC84094 at 17.39 ± 2.74 μM and NSC1011 at 30.47 ± 6.24 μM (Fig. 8). The rVAMP-2 as used in our experiment is the full length polypeptide which increases the potency of metalloprotease, simultaneously decreasing the inhibitory potential of any drug candidate. This result thus, holds higher efficacy by acting on the complete substrate which is simulating the living system.

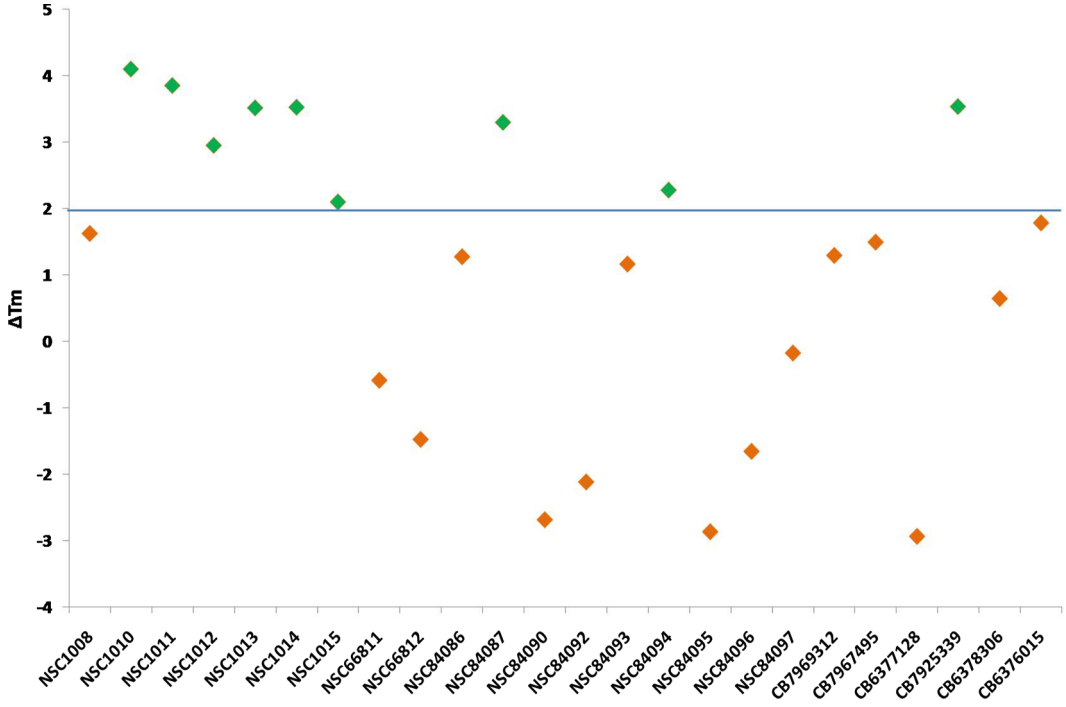


**Fig. 4.** (*continued*)

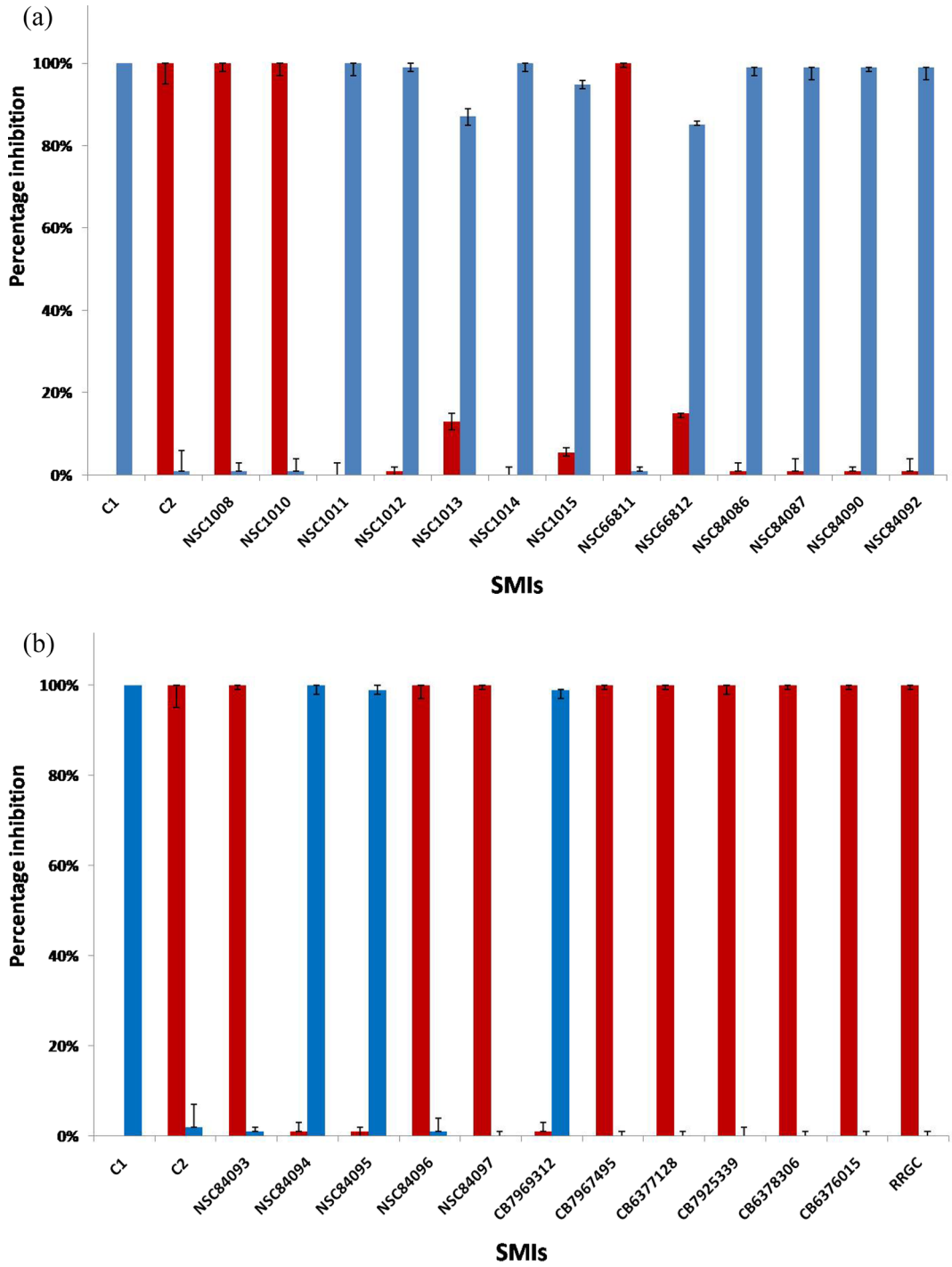


**Fig. 5.** (a and b) Percentage inhibition by small molecules screened through high through-put at 250 μM with rBoNT/F-LC at 5 nM and rVAMP-2 at 500 nM as observed through endopeptidase assay.

### 3.6. Hemolysis assay

Before moving on to *in vivo* analysis of selected compounds we performed hemolysis assay on human blood sample in order to determine hemolytic effect of SMIs. Hemolysis assay provided significant results as the hemolysis of human red blood cells was observed lower than 10% for all the compounds tested even at 100 μM concentration. The percentage obtained for NSC1011 was 3.89 ± 0.2 and 0.62 ± 0.2 for 100 and 10 μM, respectively. Similarly, NSC1014 displayed hemolytic percentage of 3.01 ± 0.3 and 0.94 ± 0.2 at 100 and 10 μM concentrations. The average hemolytic percentage of human red blood cells with NSC84094 was 5.23 ± 4 and 0.68 ± 0.001 for 100 and 10 μM, respectively (Fig. 9). The less than 10% hemolysis of human red blood cells represents good hemo-compatibility and non-toxicity against erythrocyte membranes [47].

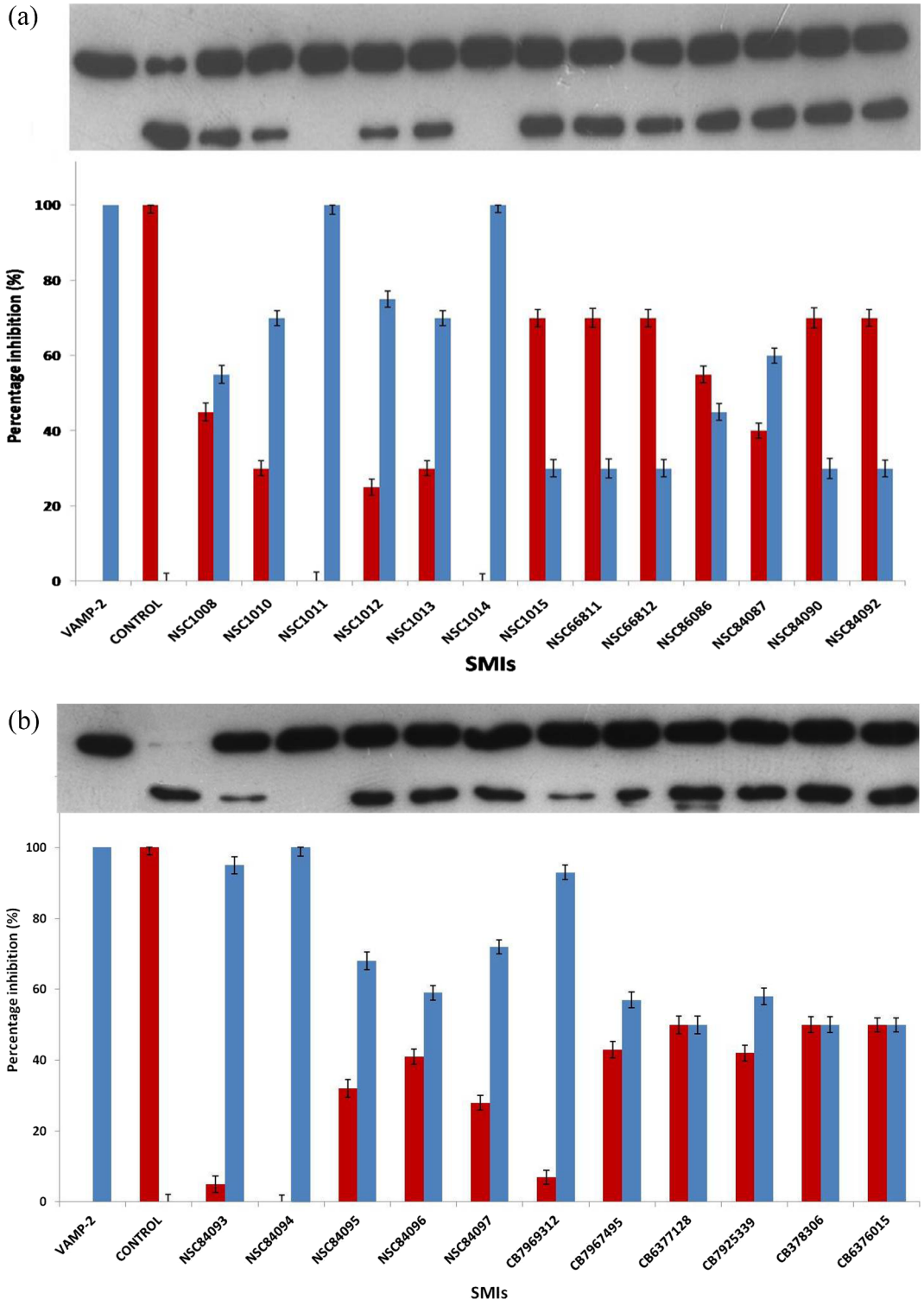


**Fig. 6.** (a and b) Selected 8-HQ based small molecules analysed through endopeptidase assay at 100 μM on rBoNT/F-LC at 5 nM and rVAMP-2 at 500 nM.

**Table 2**
SPR based determination of small molecule inhibition kinetics.

| SMI | Ka (1/Ms) | $K_d$ (1/s) | $K_D$ (M) |
|---|---|---|---|
| NSC1011 | 2.64E + 00 | 8.29E-02 | 3.14E − 02 |
| NSC1012 | 1.46E + 00 | 5.18E-02 | 3.54E − 02 |
| NSC1014 | 4.25E + 03 | 2.37E-02 | 5.58E − 06 |
| NSC84087 | 3.06E + 00 | 1.05E-01 | 3.43E − 02 |
| NSC84094 | 1.11E + 03 | 5.31E-02 | 4.79E − 05 |

### 3.7. Protection of mice against BoNT/F challenge

Two compounds NSC1011 and NSC1014 narrowed down after *in vitro* assays were evaluated in mice against BoNT/F challenge. At this stage we had to eliminate NSC84094 due to its unavailability of the molecule at required amount. No death was observed in vehicle control and all mice died between 12 and 16 h with symptoms of botulism in neurotoxin alone treated group. In *in vitro* neutralization condition no animal showed any symptoms of toxicity suggesting complete

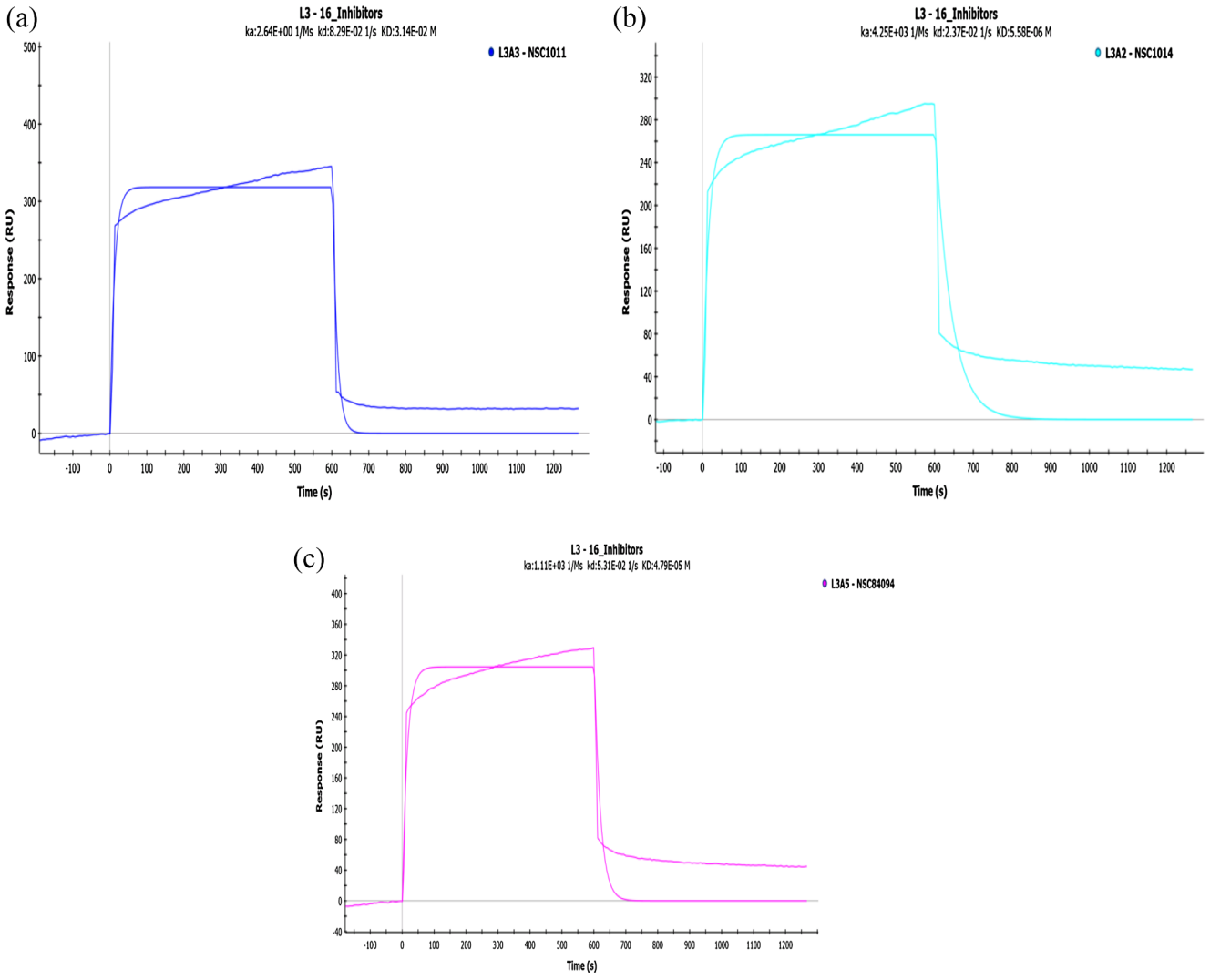


**Fig. 7.** Langmuir fitted plot of selected SMIs as observed through Proteon XPR-36 system. (a) NSC1011, (b) NSC1014 and (c) NSC84094 at 10 μM. The three selective compounds were based on previous two *in vitro* assays and NSC66812 was taken as negative control for determination of $K_D$ of the respective compounds.

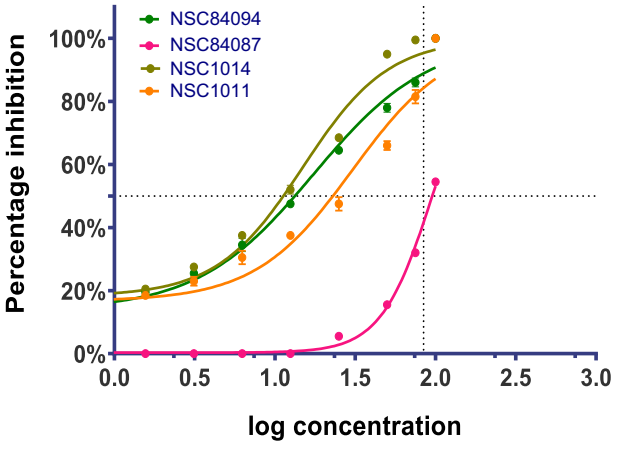


**Fig. 8.** $IC_{50}$ determination in dose-dependent manner of NSC101, NSC1014 and NSC84094. Ten concentrations 100, 75, 50, 25, 12.5, 6.25, 3.125, 1.5625, 0.78125, and 0.390625 μM of the respective small molecules were taken to determine effective $IC_{50}$ values.

protection against neurotoxin. There were no symptoms of toxicity observed in animals till the experiment concluded. In prophylactic treatment a minimal extension of 4–20 h was recorded and in therapeutic treatment, extension of survival time was recorded from 16 to 24 h (Fig. 10). Clearly, the extension in survival time in animals was comparatively higher in therapeutic than prophylactic treatment. Our findings from *in vivo* assay revealed that compounds are highly effective in neutralizing toxin in premixed condition and protecting mice against BoNT/F toxicity up to a limit in therapeutic condition.

## 4. Conclusion

This study proves the 8-HQ compounds have edge over other compounds emphasizing that the inhibitory potential of SMIs is much more complex system of cumulative inhibitory properties of the compounds. The lead identified in this study is unravelling the cascade of drug development through further SMIs designing and synthesis. The present work on these compounds paves a path towards designing and development of potent inhibitors against BoNTs that could play significant role in post warfare scenario. Our post studies will address

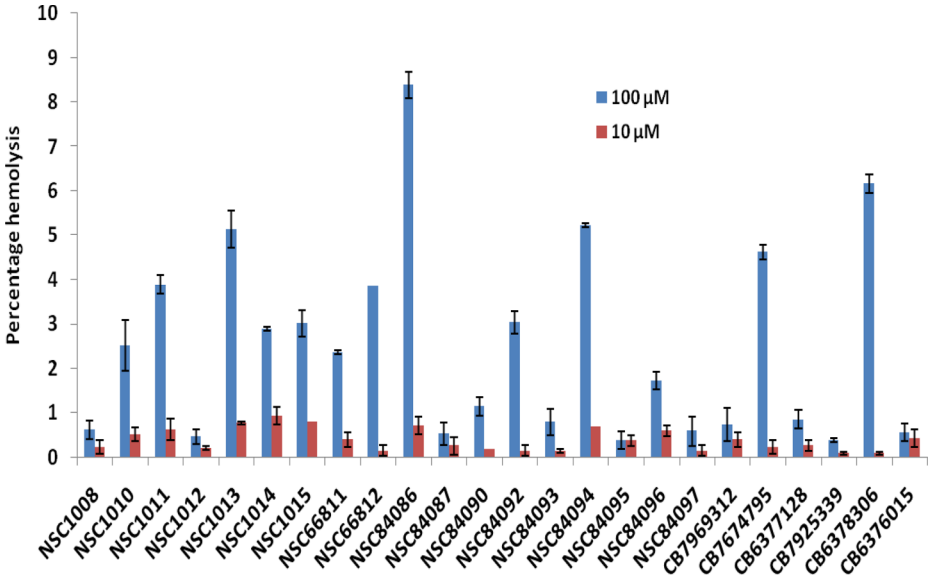


**Fig. 9.** Percentage hemolysis as calculated using the hemolytic assay formula for 100 and 10 µM concentration of 8-HQ SMIs. The hemolysis obtained from Triton-X 100 was taken as 100% hemolysis and that with respective concentration of DMSO was taken as negative control. The hemolytic percentage was observed to be below 10% for all the compounds.

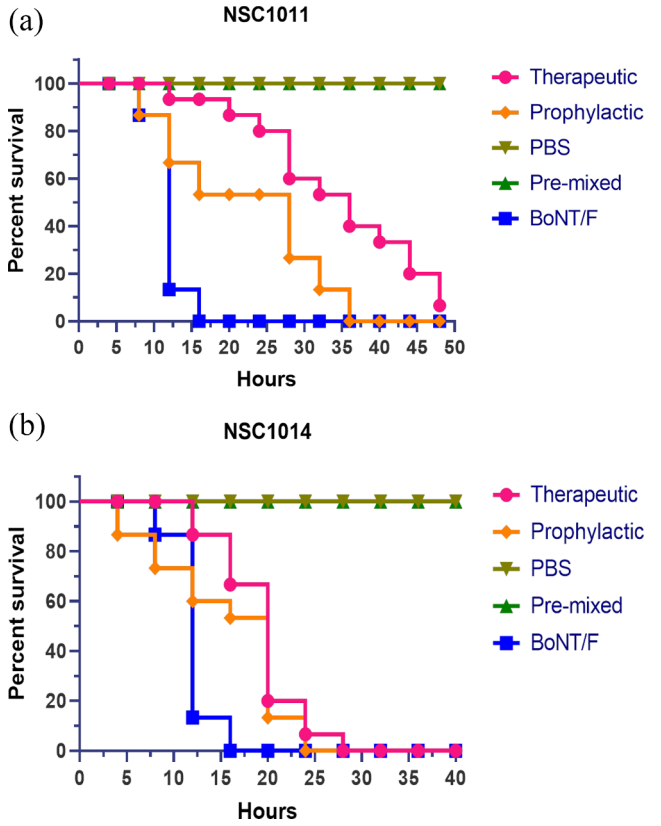


**Fig. 10.** Mouse bioassay as performed in five groups of five animals each administered with 5X MLD of ammonium sulphate precipitated BoNT/F toxin with 25 mM of inhibitors. As observed in graph NSC1011 (a) and NSC1014 (b) displaying extension in prophylactic and therapeutic condition.

these compounds one by one in order to design and in house synthesis to discover much more inhibitory derivatives through structure activity relationship.

## Acknowledgements

Authors are thankful to Director DRDE, Gwalior for providing all facilities and support required for this study. We also thank Dr Christian Leveque, INSERM, France for providing GST-VAMP-2 recombinant vector. The manuscript is internally reviewed and assigned with no. DRDE/BT/002/2019.

## Funding

The study has been internally funded by DRDE, Gwalior. Ms. Ritika Chauhan is SRF of CSIR (09/839(0016)/2015-EMR-I), Govt. of India. Dr Vinita Chauhan is RA of CSIR, Govt of India.

## Declaration of Competing Interest

The authors declare no conflicts of interest with respect to authorship for publication of this article.

## Appendix A. Supplementary material

Supplementary data to this article can be found online at https://doi.org/10.1016/j.bioorg.2019.103297.

## References

[1] Centers for Disease Control and Prevention (CDC). Botulism outbreak associated with eating fermented food–Alaska, 2001. MMWR 50 (2001) 680.
[2] L.D. Smith, Botulism, The organism, its toxins, the disease. Charles C. Thomas, 301-327 East Lawrence Avenue Springfield, Illinois 62717, USA, 1977.
[3] E.A. Johnson, M. Bradshaw, *Clostridium botulinum* and its neurotoxins: a metabolic and cellular perspective, Toxicon 39 (2001) 1703–1722.
[4] G. Schiavo, M. Matteoli, C. Montecucco, Neurotoxins affecting neuroexocytosis, Physiol. Rev. 80 (2000) 717–766.
[5] K. Oguma, Y. Fujinaga, K. Inoue, Structure and function of *Clostridium botulinum* toxins, Microbiol. Immunol. 39 (1995) 161–168.
[6] L.L. Simpson, Identification of the major steps in botulinum toxin action, Annu. Rev. Pharmacol. Toxicol. 44 (2004) 167–193.
[7] D. Dressler, F.A. Saberi, Botulinum toxin: mechanisms of action, Europ. Neurol. 53 (2005) 3–9.
[8] T.J. Smith, J. Lou, I.N. Geren, C.M. Forsyth, R. Tsai, S.L. Laporte, W. Tepp, M. Bradshaw, E.A. Johnson, L.A. Smith, J.D. Marks, Sequence variation within botulinum neurotoxin serotypes impacts antibody binding and neutralization, Infect. Immun. 73 (2005) 5450–5457.
[9] R.E. Black, R.A. Gunn, Hypersensitivity reactions associated with botulinal antitoxin, Am. J. Med. 69 (1980) 567–570.
[10] L.S. Siegel, Human immune response to botulinum pentavalent (ABCDE) toxoid determined by a neutralization test and by an enzyme-linked immunosorbent assay, J. Clin. Microbiol. 26 (1988) 2351–2356.
[11] S.S. Arnon, R. Schechter, T.V. Inglesby, D.A. Henderson, J.G. Bartlett, M.S. Ascher, E. Eitzen, A.D. Fine, J. Hauer, M. Layton, S. Lillibridge, Botulinum toxin as a biological weapon: medical and public health management, JAMA 285 (2001) 1059–1070.
[12] R. Kobayashi, T. Kohda, K. Kataoka, H. Ihara, S. Kozaki, D.W. Pascual, H.F. Staats, H. Kiyono, J.R. McGhee, K. Fujihashi, A novel neurotoxoid vaccine prevents

mucosal botulism, J. Immunol. 174 (2005) 2190–2195.
[13] S.S. Arnon, R. Schechter, S.E. Maslanka, N.P. Jewell, C.L. Hatheway, Human botulism immune globulin for the treatment of infant botulism, N. Engl. J. Med. 354 (2006) 462–471.
[14] D.B. Lacy, W. Tepp, A.C. Cohen, B.R. DasGupta, R.C. Stevens, Crystal structure of botulinum neurotoxin type A and implications for toxicity, Nat. Struct. Mol. Biol. 5 (1998) 898.
[15] B. Segelke, M. Knapp, S. Kadkhodayan, R. Balhorn, B. Rupp, Crystal structure of *Clostridium botulinum* neurotoxin protease in a product-bound state: Evidence for noncanonical zinc protease activity, Proc. Natl. Acad. Sci. U.S.A. 101 (2004) 6888–6893.
[16] M. Adler, J.D. Nicholson, B.E. Hackley, Efficacy of a novel metalloprotease inhibitor on botulinum neurotoxin B activity, FEBS Lett. 429 (1998) 234–238.
[17] S. Eswaramoorthy, D. Kumaran, S. Swaminathan, Crystallographic evidence for doxorubicin binding to the receptor-binding site in *Clostridium botulinum* neurotoxin B, Acta Crystallogr. D: Biol. Cryst. 57 (2001) 1743–1746.
[18] J.C. Burnett, J.J. Schmidt, R.G. Stafford, R.G. Panchal, T.L. Nguyen, A.R. Hermone, J.L. Vennerstrom, C.F. McGrath, D.J. Lane, E.A. Sausville, D.W. Zaharevitz, Novel small molecule inhibitors of botulinum neurotoxin A metalloprotease activity, Biochem. Biophys. Res. Commun. 310 (2003) 84–93.
[19] C. Anne, A. Blommaert, S. Turcaud, A.S. Martin, H. Meudal, B.P. Roques, Thio-derived disulfides as potent inhibitors of botulinum neurotoxin type B: implications for zinc interaction, Bioorg. Med. Chem. 11 (2003) 4655–4660.
[20] C. Anne, S. Turcaud, J. Quancard, F. Teffo, H. Meudal, M.C. Fournié-Zaluski, B.P. Roques, Development of potent inhibitors of botulinum neurotoxin type B, J. Med. Chem. 46 (2003) 4648–4656.
[21] I. Merino, J.D. Thompson, C.B. Millard, J.J. Schmidt, Y.P. Pang, Bis-imidazoles as molecular probes for peripheral sites of the zinc endopeptidase of botulinum neurotoxin serotype A, Bioorg. Med. Chem. 14 (2006) 3583–3591.
[22] G.E. Boldt, J.P. Kennedy, K.D. Janda, Identification of a potent botulinum neurotoxin a protease inhibitor using in situ lead identification chemistry, Org. Lett. 8 (2006) 1729–1732.
[23] Y.P. Pang, A. Vummenthala, R.K. Mishra, J.G. Park, S. Wang, J. Davis, C.B. Millard, J.J. Schmidt, Potent new small-molecule inhibitor of botulinum neurotoxin serotype A endopeptidase developed by synthesis-based computer-aided molecular design, PLoS ONE 4 (2009) e7730.
[24] S.T. Moe, A.B. Thompson, G.M. Smith, R.A. Fredenburg, R.L. Stein, A.R. Jacobson, Botulinum neurotoxin serotype A inhibitors: small-molecule mercaptoacetamide analogs, Bioorg. Med. Chem. 17 (2009) 3072–3079.
[25] B. Li, N.P. Peet, M.M. Butler, J.C. Burnett, D.T. Moir, T.L. Bowlin, Small molecule inhibitors as countermeasures for botulinum neurotoxin intoxication, Molecules 16 (2011) 202–220.
[26] G. Kumar, R. Agarwal, S. Swaminathan, Discovery of a fluorene class of compounds as inhibitors of botulinum neurotoxin serotype E by virtual screening, ChemComm. 48 (2012) 2412–2414.
[27] H. Seki, S. Xue, M.S. Hixon, S. Pellett, M. Remes, E.A. Johnson, K.D. Janda, Toward the discovery of dual inhibitors for botulinum neurotoxin A: concomitant targeting of endocytosis and light chain protease activity, ChemComm. 51 (2015) 6226–6229.
[28] G. Kumar, R. Agarwal, S. Swaminathan, Small molecule non-peptide inhibitors of botulinum neurotoxin serotype E: Structure–activity relationship and a pharmacophore model, Bioorg. Med. Chem. 24 (2016) 3978–3985.
[29] Y. Zhou, B.E. McGillick, Y.H. Teng, K. Haranahalli, I. Ojima, S. Swaminathan, R.C. Rizzo, Identification of small molecule inhibitors of botulinum neurotoxin serotype E via footprint similarity, Bioorg. Med. Chem. 24 (2016) 4875–4889.
[30] V. Roxas-Duncan, I. Enyedy, V.A. Montgomery, V.S. Eccard, M.A. Carrington, H. Lai, N. Gul, D.C. Yang, L.A. Smith, Identification and biochemical characterization of small-molecule inhibitors of *Clostridium botulinum* neurotoxin serotype A, Antimicrob. Agents Chemother. 53 (2009) 3478–3486.
[31] H. Lai, M. Feng, V. Roxas-Duncan, S. Dakshanamurthy, L.A. Smith, D.C. Yang, Quinolinol and peptide inhibitors of zinc protease in botulinum neurotoxin A: effects of zinc ion and peptides on inhibition, Arch. Biochem. Biophys. 491 (2009) 75–84.
[32] D. Caglic, M.C. Krutein, K.M. Bompiani, D.J. Barlow, G. Benoni, J.C. Pelletier, A.B. Reitz, L.L. Lairson, K.L. Houseknecht, G.R. Smith, T.J. Dickerson, Identification of clinically viable quinolinol inhibitors of botulinum neurotoxin A light chain, J Med. Chem. 57 (2014) 669–676.
[33] V.A. Montgomery, S.A. Ahmed, M.A. Olson, R.M. Mizanur, R.G. Stafford, V. Roxas-Duncan, L.A. Smith, *Ex vivo* inhibition of *Clostridium botulinum* neurotoxin types B, C, E, and F by small molecular weight inhibitors, Toxicon. 98 (2015) 12–19.
[34] K.M. Bompiani, D. Caglic, M.C. Krutein, G. Benoni, M. Hrones, L.L. Lairson, H. Bian, G.R. Smith, T.J. Dickerson, High-hrough-put screening uncovers novel botulinum neurotoxin inhibitor chemotypes, ACS Comb. Sci. 18 (2016) 461–474.
[35] P.T. Bremer, M. Adler, C.H. Phung, A.K. Singh, K.D. Janda, Newly designed quinolinol inhibitors mitigate the effects of botulinum neurotoxin A in enzymatic, cell-based, and *ex vivo* assays, J. Med. Chem. 60 (2017) 338–348.
[36] W.A. Harrell Jr, R.C. Vieira, S.M. Ensel, V. Montgomery, R. Guernieri, V.S. Eccard, Y. Campbell, V. Roxas-Duncan, J.H. Cardellina II, R.P. Webb, L.A. Smith, A matrix-focused structure-activity and binding site flexibility study of quinolinol inhibitors of botulinum neurotoxin serotype A, Bioorg. Med. Chem. 27 (2017) 675–678.
[37] Y.V. Minnow, R. Goldberg, S.R. Tummalapalli, D.P. Rotella, N.M. Goodey, Mechanism of inhibition of botulinum neurotoxin type A light chain by two quinolinol compounds, Arch. Biochem. Biophys. 618 (2017) 15–22.
[38] G.M. Morris, R. Huey, W. Lindstrom, M.F. Sanner, R.K. Belew, D.S. Goodsell, A.J. Olson, AutoDock4 and AutoDockTools4: Automated docking with selective receptor flexibility, J. Comput. Chem. 30 (2009) 2785–2791.
[39] E.F. Pettersen, T.D. Goddard, C.C. Huang, G.S. Couch, D.M. Greenblatt, E.C. Meng, T.E. Ferrin, UCSF Chimera—a visualization system for exploratory research and analysis, J. Comput. Chem. 30 (2004) 1605–1612.
[40] R. Chauhan, V. Chauhan, M.K. Rao, D. Chaudhary, S. Bhagyawant, R.K. Dhaked, High level expression and immunochemical characterization of botulinum neurotoxin type F light chain, Prot. Expr. Purif. 146 (2018) 51–60.
[41] V. Chauhan, D. Chaudhary, U. Pathak, N. Saxena, R.K. Dhaked, *In silico* discovery and validation of amide based small molecule targeting the enzymatic site of shiga toxin, J. Med. Chem. 59 (2016) 10763–10773.
[42] P.C. Sathler, A.L. Lourenço, C.R. Rodrigues, L.C. da Silva, L.M. Cabral, A.K. Jordão, A.C. Cunha, M.C. Vieira, V.F. Ferreira, C.E. Carvalho-Pinto, H.C. Kang, *In vitro* and *in vivo* analysis of the antithrombotic and toxicological profile of new antiplatelets N-acylhydrazone derivatives and development of nanosystems: determination of novel NAH derivatives antiplatelet and nanotechnological approach, Thromb. Res. 134 (2014) 376–383.
[43] C.D. Duarte, E.J. Barreiro, C.A. Fraga, Privileged structures: a useful concept for the rational design of new lead drug candidates, Mini-Rev. Med. Chem. 7 (2007) 1108–1119.
[44] R. Agarwal, J.J. Schmidt, R.G. Stafford, S. Swaminathan, Mode of VAMP substrate recognition and inhibition of *Clostridium botulinum* neurotoxin F, Nat. Struct. Mol. Biol. 16 (2009) 789.
[45] M.W. Pantoliano, E.C. Petrella, J.D. Kwasnoski, V.S. Lobanov, J. Myslik, E. Graf, T. Carver, E. Asel, B.A. Springer, P. Lane, F.R. Salemme, High-density miniaturized thermal shift assays as a general strategy for drug discovery, J. Biomol. Screen. 6 (2001) 429–440.
[46] C. Yung-Chi, W.H. Prusoff, Relationship between the inhibition constant (Ki) and the concentration of inhibitor which causes 50 per cent inhibition (I50) of an enzymatic reaction, Biochem. Pharmacol. 22 (1973) 3099–3108.
[47] K. Amin, R.M. Dannenfelser, *In vitro* hemolysis: guidance for the pharmaceutical scientist, J. Pharm. Sci. 95 (2006) 1173–1176.